

# THz anomalous transmission in plasmonic lattices; incidence angle dependence

Tho D. Nguyen<sup>a</sup>, Ajay Nahata<sup>b</sup> and Z. Valy Vardeny<sup>a</sup>

<sup>a</sup>Department of Physics and Astronomy, University of Utah, Salt Lake City, Utah 84112, USA

<sup>b</sup>Department of Electrical and Computer Engineering, University of Utah, Salt Lake City, Utah 84112, USA

## Abstract

The phenomenon of anomalous transmission through subwavelength aperture arrays in metallic films (plasmonic lattices) is thought to be mediated by surface plasmon polaritons (SPP) on the film surfaces. Using terahertz time-domain spectroscopy we systematically studied the anomalous transmission spectrum through plasmonic lattices as a function of the incidence angle,  $\theta$  of the impinging beam. We observed splitting of the various transmission resonances into two resonance branches when  $\theta$  deviates from normal incidence that depends on the polarization direction of the beam respect to the plane of incidence and  $\theta$ . We show that the transmission resonance splitting is not related to dispersion relation of different SPP branches, but rather is associated to the interference properties of the SPP waves on the metal surface. The dependence of the split resonant frequencies vs.  $\theta$  is fit with a theoretical formula that takes into account the *effective dielectric function* of the plasmonic lattice vs.  $\theta$ , which emphasizes the important role of the Fano-type anti-resonances in the transmission spectrum. Finally, we introduced a simple way for making an efficient notch filter with high Q factor exploiting the splitting of transmission resonance under rotation.

**Keywords:** Keywords: THz radiation, anomalous transmission, plasmonic lattice, light polarization, effective dielectric response, notch filter

## 1. INTRODUCTION

Extraordinary transmission (EOT) of light through periodic/apperiodic perforated metal films with subwavelength apertures (plasmonic lattices) has been extensively studied in the past decade [1-6]. Recently, there has been growing interest in studying the dielectric response of the lattices, which is of fundamental importance in determining the propagation properties of electromagnetic waves. Based on the approximation that metals are perfect conductors, Pendry and coworkers [7,8] recently proposed a theoretical framework hypothesizing that metallic films perforated with periodically spaced apertures exhibit an *effective* plasma response ('sp spoof plasmons'), which is approximated by the cut-off frequency of the waveguide mode in the individual apertures. Using THz time-domain spectroscopy (THz-TDS) of both random and periodic hole arrays, Agrawal et. al. [9] experimentally extracted both amplitude and phase information [10-12], which were used for calculating the effective dielectric response  $\epsilon(\omega)$  of the aperture arrays [13]. It was found that  $\epsilon(\omega)$  consists of a superposition of an effective 'plasma-like' response that is associated with the *uncorrelated* individual apertures, superimposed by discrete resonances associated with the launched SPP interference on the metal surface, that are consequently related to the reciprocal vectors of the underlying aperture arrays in the Fourier space. Following the model proposed by Agrawal et al [9], we systematically study in this submission the effective dielectric response of a free standing plasmonic lattice as a function of polarization and incidence angle,  $\theta$  of the impinging beam. We fit the data by an angle dependent effective dielectric function, and show that is in fact also polarization dependent. Finally, we propose a simple way to achieve an efficient notch filter using multiple plasmonic lattices of known dielectric response in tandem.

## 2. EXPERIMENTAL

For our studies we fabricated periodic and a random array of subwavelength apertures on 75  $\mu\text{m}$  thick freestanding stainless steel metallic films. For the polarization and incident angle dependencies of the impinging electromagnetic THz beam, we used periodic apertures that were arranged in a square lattice with a lattice constant of 1.5 mm and aperture

diameters of 600  $\mu\text{m}$ . For the multiple periodic hole array studies, the square lattices had a lattice constant of 1 mm and aperture diameters of 500  $\mu\text{m}$ , 600  $\mu\text{m}$  and 700  $\mu\text{m}$ , respectively. The samples were placed in the THz beam at various angle with respect to the incident beam so that both the polarization and incident angle could be easily changed (see Fig. 1 insets). The random aperture array with holes of 600  $\mu\text{m}$  diameter was designed such that it had the same fractional aperture area with the corresponding plasmonic lattice having the same hole diameter. Two dimensional (2D) Fourier transforms applied to the random aperture arrays pattern did not yield any discrete peaks in the reciprocal space, confirming that the aperture distribution in these samples was truly random.

We used a conventional time-domain THz spectroscopy setup [10] for characterizing the 2D aperture arrays. Photoconductive devices were used for both emission and coherent detection. An off-axis paraboloidal mirror was used to collect and collimate the THz radiation beam from the emitter to the samples. The samples were attached to a solid metal plate with a 5 cm x 5 cm opening that is significantly larger than the THz beam size, which was placed in the path of the collimated THz beam. The detected transient photocurrent,  $\text{PC}(\tau)$  was recorded as a function of the translation stage path that determined the time delay,  $\tau$  between the ‘pump’ beam that hits the emitter and the ‘probe’ beam that arrives at the detector.  $\text{PC}(\tau)$  was Fourier transformed and normalized to the reference transmission, yielding both the electric field transmission *magnitude and phase*,  $t(\omega)$  in the range  $\sim 0.05$  THz to 0.6 THz. The resulting Fourier transformed data may be described by the relation:

$$t(\omega) = |t(\omega)| \exp[\varphi(\omega)] = \frac{E_{\text{transmitted}}(\omega)}{E_{\text{incident}}(\omega)}, \quad (1)$$

In this expression,  $E_{\text{incident}}$  and  $E_{\text{transmitted}}$  are the incident and transmitted THz fields, respectively,  $|t(\omega)|$  and  $\varphi(\omega)$  are the magnitude and phase of the amplitude transmission coefficient, respectively, and  $\omega/2\pi$  is the THz frequency.

The incident THz beam normal to the aperture array plane was consider to be at zero rotation angle, namely  $\theta = 0$ . The rotation axis was on the array plane, either in the vertical or horizontal direction, see below.

### 3. RESULTS AND DISCUSSION

We first studied the polarization effect on the anomalous transmission spectra. The array position was set normal respect to the incident THz beam so that its polarization is either parallel to the (1,0) or (1,1) directions. Subsequently the arrays were rotated around either horizontal or vertical axis. Fig. 1 shows the transmission spectra through a periodic hole array with 1.5 mm lattice spacing and 600  $\mu\text{m}$  hole diameter as a function of polarization, rotation angle and  $\theta$ . In particular, in Fig. 1(a) and 1(b), the THz beam polarization is set along two different directions, namely (1,0) and (1,1) direction. The rotation axes in each case are in the same direction as that of the polarization. In contrast the rotation axes are perpendicular to the beam polarization in Fig. 1(c) & 1(d). The dash line in Fig. 1(a) shows the transmission spectrum of a random aperture array having similar hole diameter of 600  $\mu\text{m}$  as in the periodic arrays. Its transmission spectrum does not change with the incident angle. In contrast, the fundamental (1,1) (Fig. 1(a)) and (1,0) (Fig. 1(b)) SPP resonance, at  $\sim 0.27$  THz and  $\sim 1.9$  THz, respectively, each splits into two frequency branches [1,9]. We note that the transmission resonance frequencies in the periodic array are robust if the rotation axis coincides with the corresponding reciprocal vector direction of the resonance. This is seen in Figs. 1(c) and 1(d). When the rotation axis does not coincide neither with (0,1) nor with (1,1) directions, then both resonance frequencies that correspond with these reciprocal vectors split into two branches. In summary all transmission spectra in Fig. 1 may be viewed as a superposition of two transmission components: (i) a broad spectrum, which relates to the transmission through individual holes and is insensitive with the incident angle and polarization; and (ii) a discrete resonance spectrum, which strongly depends on the incident angle and polarization.

In order to better understand the transmission spectra in Fig. 1(a) we assume that the aperture array behaves as an effective medium in the THz beam path and, therefore, could directly obtain the dielectric response,  $\epsilon(\omega)$  of the perforated metal films, without resorting to the traditional Kramers-Kronig transformation, where somewhat arbitrary assumptions about asymptotic behavior are usually made. Figures 2(a) and 2(c) show the real and imaginary components

of the dielectric constant,  $\epsilon(\omega)$  of the arrays which were calculated from the corresponding transmission amplitude and phase spectra in Fig 1(a) & 1(b), respectively. We found that  $\epsilon(\omega)$  of the periodic array can be well described by a superposition of a non resonant and resonant components given by the formula [9,14,15]:

$$\tilde{\epsilon}(\omega) = \epsilon_{\infty} \left( 1 - \frac{\tilde{\omega}_p^2}{\omega^2 + i\gamma\omega} \right) + \sum_j r_j \frac{\omega_{Lj}^2 - \omega^2}{\omega_{Rj}^2 - \omega^2 - i\gamma_j\omega} + \dots \quad (2)$$

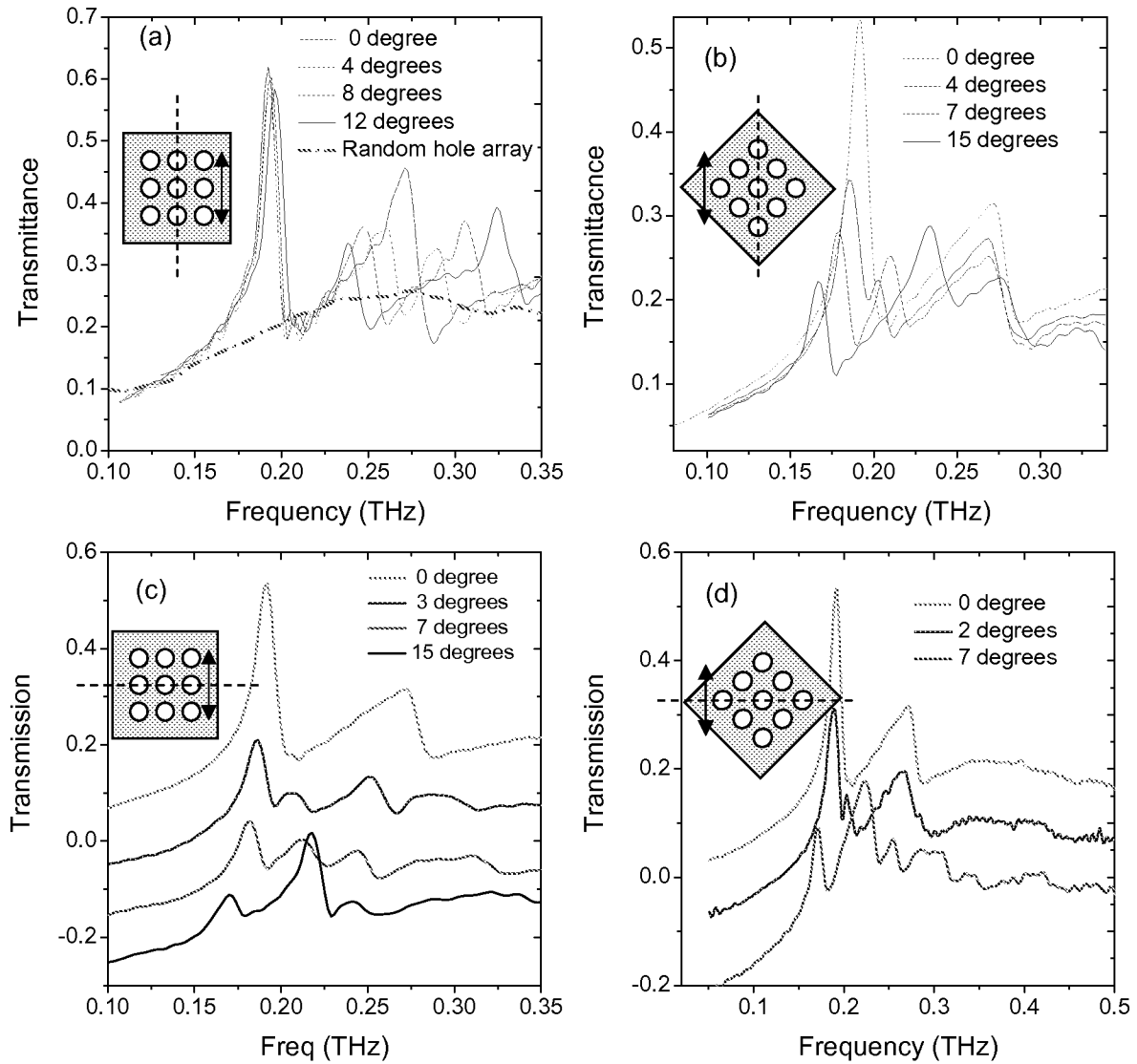


Figure 1. Incident polarization and angle dependent transmission studies of a stainless steel foil perforated with periodic aperture arrays having  $D = 600 \mu\text{m}$  and dimeter lattice constant  $a = 1.5 \text{ mm}$ . The insets shows the incident polarization (two-direction arrows), and the rotational axes (dash lines). The transmission through a random aperture array having the same aperture diameter and overall fractional aperture area as the studied plasmonic lattice is shown in (a) as a dashed-dotted line. The fundamental (1, 0) and (1, 1) SPP resonances at  $\sim 0.19$  and  $\sim 2.7$  THz, respectively each splits into two resonance branches depending on the incident polarization and rotation axis. The transmission of the random aperture arrays shown in (a) does not depend on polarization, rotation axis or impinging angle.

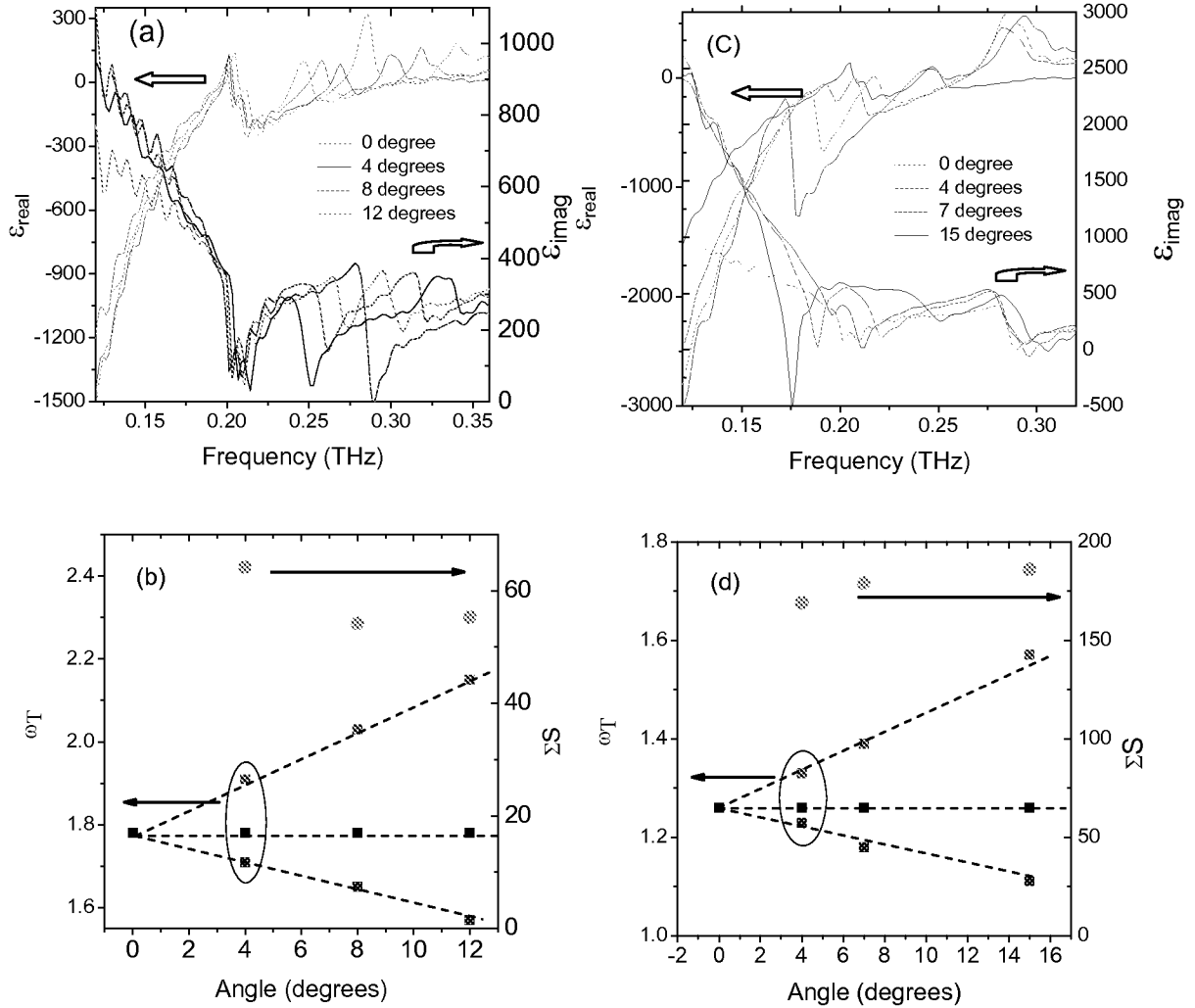


Figure 2. (a) and (c) The spectra of the real (left axis) and imaginary (right axis)  $\epsilon(\omega)$  components obtained from the transmission spectra of Fig 1(a) & 1(b) at various  $\theta$ . The dielectric response was obtained by fitting the data using equation (1). The fitting parameters,  $\omega_T$  and  $\Sigma S$  (see text) are shown in (b) and (d) as a function of  $\theta$  and correspond to  $\epsilon(\omega)$  shown in (a) and (c), respectively. The corresponding dash lines through the data points are guide to the eye.

The first term is a plasma-like, non resonant dielectric response, where  $\tilde{\omega}_p$  is the *effective* plasma frequency that is set by the cut-off frequency,  $f_c$  of a cylindrical aperture given by  $f_c = ca_m/\pi D$ , where  $a_m$  is a mode-dependent constant  $\sim 1.841$  for the lowest-order mode (TE<sub>11</sub>), and  $c$  is the speed of light [16];  $\epsilon_\infty$  is the high frequency dielectric constant, and  $\gamma$  is the plasma relaxation rate. The second term in Eq. (2) is the resonant component that depends on the particular SPP resonance in the plasmonic lattice; this component varies with polarization and incident angle of the impinging beam. Here  $\omega_{L_j}$  and  $\omega_{T_j}$  are the effective longitudinal optical (LO) and transverse optical (TO) frequencies associated with the ‘phonon-like’ resonant contribution in the effective medium, and  $\gamma_j$  is the relaxation rate (linewidth) of the  $j$ th resonance. We introduce the weighting interference factor,  $r_j$  which depends on the polarization direction and is 1/4 for each direction, (1,0) or (1,1). the dielectric function in Eq. (2) is consistent with a Fano-type interference between a continuum spectrum given by the first term and the discrete lines [6,17,18]. The maxima obtained in the transmission

spectrum are typical features of ‘LO-type’ resonances, whereas  $\omega_{T_j}$  in Eq. (2) are the antiresonance (AR<sub>i</sub>) frequencies that correspond to the dips in the transmission spectra that correspond to the various SPP branches. For fitting the obtained dielectric response using Eq. (2), we chose  $\tilde{\omega}_p \sim 1.42 \text{ s}^{-1}$  and  $\epsilon_\infty \sim 530$ , which were obtained previously from fits of  $\epsilon(\omega)$  of the random aperture array [9] whereas the TO frequencies ( $\omega_{T_j}$ ) for the resonant contribution in Eq. (2) correspond to the  $(\pm 1, 0)$  and the  $(\pm 1, \pm 1)$  plasmonic branches, which can be derived from the standard SPP model [1]. In Figs. 2(b) and 2(d) we show the best fitting values of  $\omega_{T_j}$  that we obtained from  $\epsilon(\omega)$  at various incident angles. The  $\omega_{T_j}$  values in Fig. 2(b) & 2(d) are in good agreement with the anti-resonances, or dips in the transmission spectra of Fig. 1(a) and 1(b), respectively; they definitely do not correspond to the peaks in the transmission spectra.

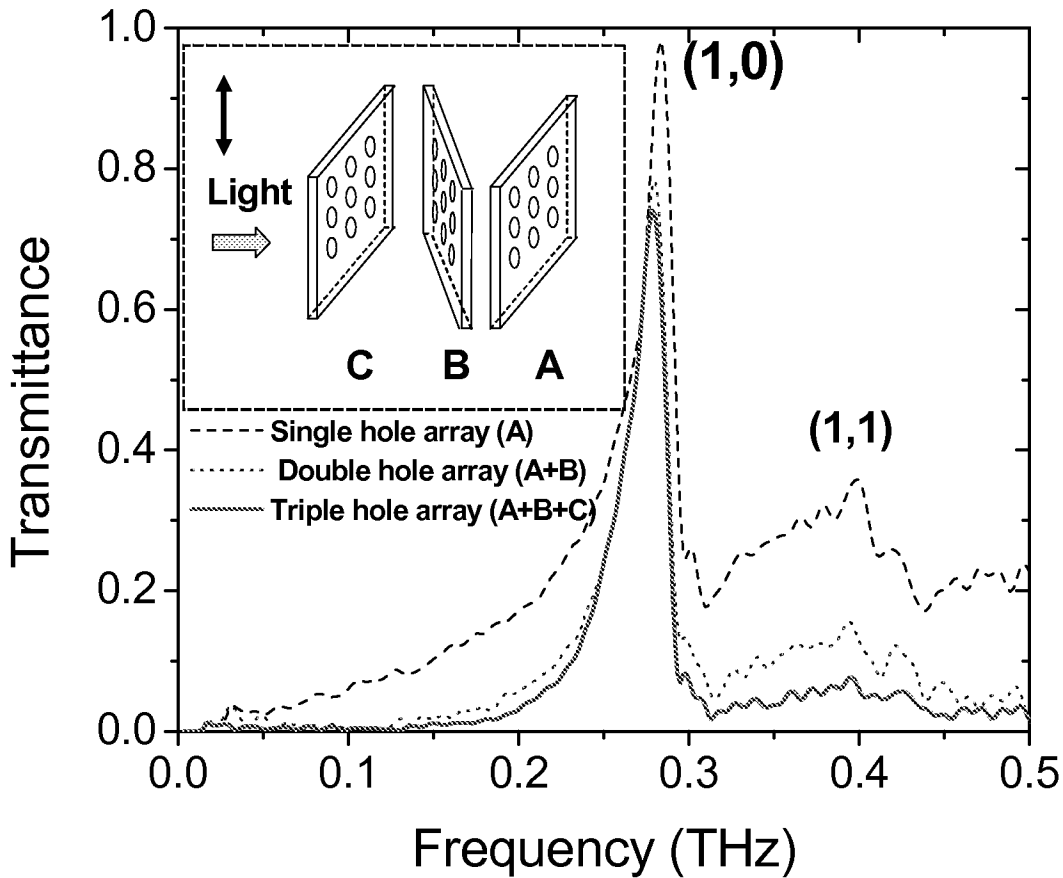


Figure 3. Transmission on multiple hole arrays in tandem, having the same lattice constant of 1 mm, but different hole diameters: A (700  $\mu\text{m}$ ), B (600  $\mu\text{m}$ ) and C (500  $\mu\text{m}$ ). The dashed line is the transmission of a single hole array C, where the incident THz is perpendicular to the array. The incident beam polarization is in the (1,0) direction. The dotted line is the transmission of a two array structure in tandem formed by adding a second array (B), which is rotated 5° from the perpendicular direction of the incident beam.. The lowest order transmission peak (1,0) remains the same, while the other peak split into two small branches and thus the transmission in that frequency range is lower. By adding the third array (A), the transmission background and the higher order resonant (1,1) band continue to be suppressed (solid line). The inset shows the physical arrangement of the multiple arrays, where the doubled-side arrow indicates the incident beam polarization direction.

We further calculated the oscillation strength,  $S_j$  [9] of the individual resonances, which is given by the relation:  $S_j = (\omega_{Lj}^2 - \omega_{Tj}^2) / \omega_{Tj}^2$ . As seen in Figs. 2(b) and 2(d) we found that the sum,  $\sum S_j$  is insensitive with the rotation angle, in agreement with previous reports [9].

In the following we describe how the interesting characteristic properties of the of transmission dependence on the beam polarization and incident angle may be used in an application, namely to create a notch/bandpass filter. In principle, the rotation of a periodic hole arrays causes a split of a particular resonant transmission peak into two peaks with substantially reduced intensities, while maintaining the transmission strength of the other resonant band. Based on this principle, a large transmission efficiency and high Q-factor notch filter may be obtained using multiple hole arrays by suppressing the transmission background of the continuous component caused by the individual holes) Fig. 3 shows the transmission spectra through single, double and triple periodic hole arrays. These stacked plasmonic lattices were composed by three hole arrays with the same periodicity of 1 mm but different hole diameters, namely A (500  $\mu\text{m}$ ), B (600  $\mu\text{m}$ ), and C (700  $\mu\text{m}$ ). The distance between the plasmonic lattice structure pairs was set to be about 4 cm. By rotating the hole array (B) around its vertical axis, it is possible to split the higher order transmission peak (1,1) of this structure, and this reduces the transmission at that frequency, and consequently this may further filter the transmission of the (1,0) band by the third array (A). This process keeps the properties of the lowest-order transmission peak intact, and therefore the Q-factor of the engineered optical filter increases with the number of plasmonic lattice structures involved. When optimally designed, the transmission efficiency of the optical filter can approach 100% with very high Q-factor at the designed frequency.

#### 4. CONCLUSIONS

We have systematically studied the anomalous transmission spectrum through plasmonic lattices as a function of polarization and the incidence angle,  $\theta$  of the impinging beam in the frequency range from  $\sim 0.05$  THz to 0.6 THz using the THz time-domain method. We observed splitting of the various transmission resonances, each into two resonance branches when  $\theta$  deviates from normal incidence, depending on the polarization direction of the beam. We studied this phenomenon in the context of an effective complex dielectric response for the arrays. The dielectric function,  $\epsilon(\omega)$  is fundamental for understanding the complete linear propagation properties of electromagnetic radiation in plasmonic lattices, and since the THz experiment can get information on both transmission amplitude and phase, we were able to determined both real and imaginary components of  $\epsilon(\omega)$  simultaneously from the same data. We found that  $\epsilon(\omega)$  consists of a superposition of an effective ‘plasma-like’ response associated with the uncorrelated apertures, and another component that is composed of discrete resonance response associated with the reciprocal lattice vectors of the underlying aperture arrays in the Fourier space. This emphasizes the important role of the Fano-type anti-resonances in the transmission spectrum. Finally, we introduced a simple way for engineering an efficient notch filter with high Q-factor by exploiting the split and reduction of the transmission resonances upon rotation, and using several plasmonic structures in tandem.

#### Acknowledgements

We acknowledge useful discussions with Dr. Agrawal. This work was supported in part by NSF-ECCS Grant No. 08-01965 at the University of Utah.

#### REFERENCES

- [1] T.W. Ebbesen *et al.*, “Extraordinary optical transmission through sub-wavelength hole arrays”, *Nature* (London) **391**, 667 (1998).
- [2] L. Martin-Moreno *et al.*, “Theory of Extraordinary Optical Transmission through Subwavelength Hole Arrays” *Phys. Rev. Lett.* **86**, 1114 (2001).
- [3] W. L. Barnes *et al.*, “Surface Plasmon Polaritons and Their Role in the Enhanced Transmission of Light through Periodic Arrays of Subwavelength Holes in a Metal Film”, *Phys. Rev. Lett.* **92**, 107401 (2004).

- [4] R. Gordon *et al.*, “Strong Polarization in the Optical Transmission through Elliptical Nanohole Arrays”, *Phys. Rev. Lett.* **92**, 037401 (2004).
- [5] H. J. Lezec *et al.*, “Beaming Light from a Subwavelength Aperture”, *Science* **297**, 820 (2002).
- [6] Matsui, T., Agrawal, A., Nahata, A. and Z. V. Vardeny,. “Transmission resonances through aperiodic arrays of subwavelength apertures”, *Nature* **446**, 517-521 (2007).
- [7] J. B. Pendry, L. Martin-Moreno, and F. J. Garcia-Vidal, “Mimicking surface plasmons with structured surfaces”, *Science* **305**, 847-848 (2004).
- [8] F. J Garcia-Vidal *et al.*, “Surfaces with holes in them: new plasmonic metamaterials”, *J. Opt. Pure Appl. Opt.* **7**, S97-S101 (2005).
- [9] A. Agrawal *et al.*, “Engineering the dielectric function of plasmonic lattices”, *Opt. Express* **16**, 9601-9613 (2008)
- [10] H. Cao and A. Nahata, “Resonantly enhanced transmission of terahertz radiation through a periodic array of subwavelength apertures”, *Opt. Express* **12**, 10041-10047 (2004).
- [11] J. Gomez-Rivas, C. Schotsch, P. Haring-Bolivar, and H. Kurz, “Enhanced transmission of THz radiation through subwavelength holes”, *Phys. Rev. B* **68**, 201306 (2003).
- [12] D. Qu, D. Grischkowsky, and W. Zhang, “Terahertz transmission properties of thin, subwavelength metallic hole arrays”, *Opt. Lett.* **29**, 896-898 (2004).
- [13] Tsong-ru tsai *et al.*, “terahertz time-domain spectroscopy studies of the optical constants of the nematic liquid crystal 5cb”, *Appl. Opt.* **42**, 2372-2376 (2003).
- [14] N. W. Ashcroft and N. D. Mermin, [*Solid State Physics* ], Saunders College, (1976).
- [15] E. L. Albuquerque and M. G. Cottam, [*Polaritons in Periodic and Quasiperiodic Structures*], Elsevier B.V. (2004).
- [16] N. Marcuvitz, [*Waveguide Handbook* ], McGraw-Hill, (1951).
- [17] C. Genet, M. P. van Exter, and J. P. Woerdman, “Fano-type interpretation of red shifts and red tails in hole array transmission spectra”, *Opt. Commun.* **225**, 331-336 (2003).
- [18] U. Fano, “Effects of configuration interaction on intensities and phase shifts”, *Phys. Rev.* **124**, 1866-1878 (1961).